Arch. Metall. Mater. **69** (2024), 1, 343-346

DOI: https://doi.org/10.24425/amm.2024.149099

J. NABIAŁEK[1], T. JARUGA[1*]

# NUMERICAL MODELLING OF MICROCELLULAR FOAMING INJECTION MOULDING

The results of computer modelling of an injection moulding process with microcellular foaming (MuCell®) were presented in this work. The process is based on the dissolving nitrogen in a liquid polymer which is possible when nitrogen is in supercritical fluid state (SCF). After pressure drop of the melt in the injection mould the intensive nucleation of pores occurs and, as the result, the material with high concentration of small pores is created. The pores obtained in this way are of much smaller size than in a conventional foaming process. The pore size in the cross-section of an exemplary injection moulded part was calculated in the computer modelling and compared to the results of microscopical investigation made on the real injection moulded part. It was found that the size of the pores depends on the flow length inside the injection mould and on the position in the part's cross-section.

*Keywords:* modelling; simulation; injection moulding; Moldflow; MuCell®

## 1. Introduction

Microcellular foaming of plastics is a technological process conducted with the use of atmospherical gases (especially nitrogen and carbon dioxide). The gases are transferred into the supercritical fluid phase (SFC) and mixed with molten plastic. In SFC the gases are of high diffusion rate, low viscosity and low surface tension and they can dissolve in liquid plastic easily. As the result, many small pores are created in the material and, when solidifying, the porous plastic is characterized with the high concentration of pores, significantly smaller as in the classical techniques of plastics foaming process (using chemical or physical porous agents). The porosity of material can be an advantage regarding the possibility of part weight reduction, which is especially important in the automotive industry. The part cost reduction is also an important issue [1] but this kind of parts should be designed with regard of easy identification, recyclability and disassembling of components of an complex product, which generally means an eco-design challenge [2]. The concept of plastics microcellular foaming technology was elaborated by Massachusetts Institute of Technology and later developed by Trexel Inc. MuCell® is a registered trademark of Trexel company [3].

### 1.1. Microcellular injection moulding

It is possible to introduce the nitrogen or $CO_2$ into a molten polymer in the injection moulding machine but a special machine construction is required. The gas in supercritical state is injected into the plasticizing unit and, in order to keep the pressure, the zone of mixing with the liquid polymer is closed by two valves. After preparing the material ready for injection (by the screw rotation in the barell) the valves are opened and the screw transfers the mixture into an injection mould. In the mould, when the pressure drops, the gas is transferred into the classical gas phase and the pores are created in the plastic. The parameter of pressure is critical in the formation of the porous structure but the temperature of plastic is also important. The injection speed can also affect the size and distribution of micropores [4]. The gas solubility in the polymer also impacts the porous structure as well as the gas content which can be different in the process. The application of nitrogen is more common in MuCell® than application of $CO_2$ since the control of the process and porous structure formation is easier with nitrogen although carbon dioxide is better soluble to polymers [1]. Generally, the mould design for microcellular injection moulding requires no significant modifications but it is possible to control the foaming process better with pressure and temperature sensors in the

[1] CZESTOCHOWA UNIVERSITY OF TECHNOLOGY, FACULTY OF MECHANICAL ENGINEERING AND COMPUTER SCIENCE, 21 ARMII KRAJOWEJ AV., 42-201 CZESTOCHOWA, POLAND

* Corresponding author: tomasz.jaruga@pcz.pl

mould cavity and using gas ($N_2$ or $CO_2$) pump connected to the mould. The size and pore distribution can be then controlled by counterpressure of a gas delivered into the mould cavity which can put the resistance on the flowing molten plastic. Without the countepressure size of the pores is non-uniform and some big-size pores occur. However, when the counterpressure exceeds a critical value, no porous structure is created [5].

### 1.2. Properties of microcellular parts materials

The properties of microporous parts, when compared to the non-porous parts of the same plastic, are different. First of all the porous material density (apparent density, because of pores) is smaller and this can be the advantage, when considering the demands of some industries, like automotive, regarding part mass reduction. On the other hand, mechanical properties are also impacted by the porosity [6] and those are deteriorated. For example, tensile strength and tensile modulus decrease with the gas content in the material, which was proved in the case of polyamide and glass fibre composite, microfoamed with nitrogen [7]. The disadvantage of foaming process is more poor surface quality because the existence of pores near part skin (product surface) increases the surface roughness. However, as reported in [8,9] a smooth surface of MuCell® injection moulded parts can be obtained in InduMold process, by rapid heating of the mould with the use of induction heating means.

More predictable foamed structure can be obtained for non-filled polymers in microcellular foaming process of injection moulding [10]. It is possible to process also reinforced plastics in this way but the filler particles can influence the pores creation and, on the other hand, the pores can impact the orientation of fillers, like glass fibres [11]. In both types of plastics, reinforced and non-filled, the structure of the material differs in the cross-section [12,13]. It is possible that in the centre (in the middle of part cross-section) some pores can join and create bigger pores in the structure [11]. There were also trials to microfoam plastics with nanofillers, like for example nanoclay particles. It was found that in this case the nanoparticles can surround the created micropores [14]. The cell density can be also increased by some additives. As reported in [15] the addition of 1,3:2,4-bis-O-(4-methyl benzylidene)-D-sorbitol gelling agent (MDBS) to polypropylene as reinforcement increased the porosity but also the tensile strength of the obtained material.

The microcellular foaming injection moulding process can contribute not only to some improvements of part quality, like smaller deformations and better surface flatness of the part, but also can cause the decrease in production costs [16].

## 2. Experimental

The modelling of microcellular injection moulding process of a polypropylene glass-fiber filled part was made using Autodesk Moldflow Insight software. The results of simulation – pore size distribution in the cross-section were compared for different places of this long flow path part. The computer simulation results were also compared to the images from the microscopical observation of the samples taken from the real part manufactured on the injection moulding machine equipped with the microcellular foaming injection unit.

### 2.1. Modelling of microcellular injection moulding

The results of modelling of the injection with MuCell® technology are presented. The molding part used for the simulation was a channel for drain water. This injection part was of the average wall thickness: 2.7 mm and the main dimensions: length: 515 mm and width: 82 mm. There was just one injection point in the mould, positioned in the middle of the part's length and it was at the end of a sprue-type gate.

The 3D model of the part, prepared in a CAD software and exported as STP file, was opened in Autodesk Moldflow Insight software and prepared for the computer simulation of microcellular injection moulding process by generation of the finite element mesh, representing the shape of the mould cavity and sprue gate.

The conditions of the injection process, assumed for the calculations, were the same as those used on the injection moulding machine:

- melt temperature: 240°C,
- mould temperature: 40°C,
- holding time: 10 s,
- cooling time: 20 s,
- holding pressure: 15 MPa,
- injection time: 2.5 s.

In addition, the following parameters were adopted for the MuCell® technology in the simulation process:

- the assumed decrease in the part mass: 10%,
- initial bubble diameter 0.001 mm,
- initial estimative bubble concentration: $2 \cdot 10^5$ 1/cm$^3$.

The injected material was polypropylene reinforced with glass fibres (30%) – Hostacom PP 2062.

### 2.2. Microscopical investigation

Small samples were cut out of the real injection moulded part. The samples were mounted on the rotary microtome Thermo Finesse ME+ and the cross-section were prepared for the microscopical investigation by microtoming on a steel solid knife. After that the cross-sections were observed on Nikon SMZ 800 optical microscope.

## 3. Results and discussion

The simulation results: pore (named in the simulation software as "bubble") size distribution at the end of the forming inside

the mould cavity in different areas of the part are presented in Fig. 1 and Fig. 3. The structure across part's thickness was observed on the microscope in the same points as defined for the simulation analysis. The microscopical photos are presented in Figs. 2 and 4.

First, the comparison of the pore size at the beginning and the end of the flow path was made. The structure of the material was compared in two points of different flow length: point 1: 10 mm from the injection point (sprue gate) and point 2: 245 mm from the injection point, measuring along the part (Fig. 1). In fact, point 2 was chosen to check the structure in the area of the end of the flow. The simulation results show not only bigger pore size at the end of the flow (0.068 mm in the middle of the thickness while near the sprue this value is about 0.05 mm) but also a local peak in the pore size near the part wall (near the skin). The average pore size difference is easy to explain because the pressure of the molten plastic drops along the flow direction and the formation of pores is easier then. The formation of bigger pores near the part wall can be explained, for example, by intensive shearing between the molten core in the middle of the cavity width (part thickness) which can lead to local temperature decrease in this point. The microscopical observations of the real case (Fig. 2) confirmed the trend recorded in the simulation: big size pores occurred mostly in the middle of the thickness in the gate area of the part ("A" zone in Fig. 2a) while two zones of big size pores were observed at the end of the flow ("B" zones in Fig. 2b). However, the zones of big pores were observed to be closer to the middle of the thickness than in the case of the simulation results (the peak was on the coordinate of 0.85 – Fig. 1)

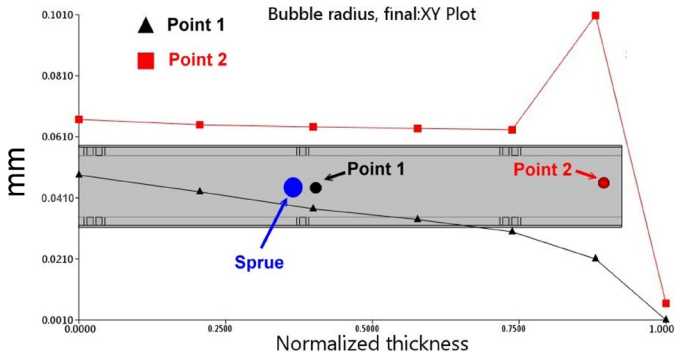


Fig. 1. The comparison of the bubble (pore) radius distribution near the sprue (point 1) and at the flow end (point 2) at different depth across the wall thickness. 0 – the middle of the thickness, 1 – part skin

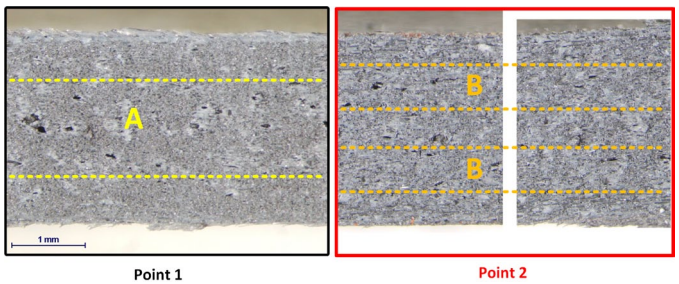


Fig. 2. The cross-section of the MuCell® part prepared on the microtome – points 1 and 2 as in Fig. 1. The areas of big size pores: A – in the middle of the thickness (point 1), B – closer to the part skin (point 2)

Another pair of points was selected for the comparison: point 3: 10 mm from the gate and point 4: 100 mm from the gate, but this distance was measured the perpendicular direction to the part' length (Fig. 3). The pore size distribution recorded in the simulation is more similar for these two points as in the microscopical images (Fig. 4). The real structure is characterized by significantly bigger pores in the middle of the thickness (point 4 – Fig. 4b) in the area further from the injection point. This can be explained by pressure drop along the flow length. The pores are bigger than in point 2. The reason of this difference can be the temperature of the melt which is higher in a place located closer to the gate and lower viscosity of the melt is an factor enabling the pore formation. The difference between simulation results and microscopical investigation can lead to conclusion that the temperature influence on microfoaming can be underestimated in the simulation algorithm.

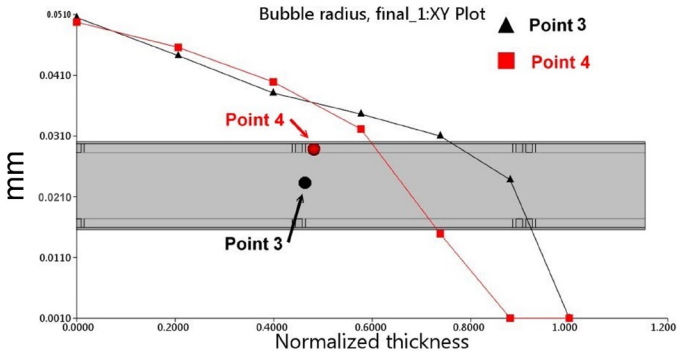


Fig. 3. The bubble (pore) radius distribution near the sprue at different depth across the wall thickness. 0 – in the middle of the thickness, 1 – part skin

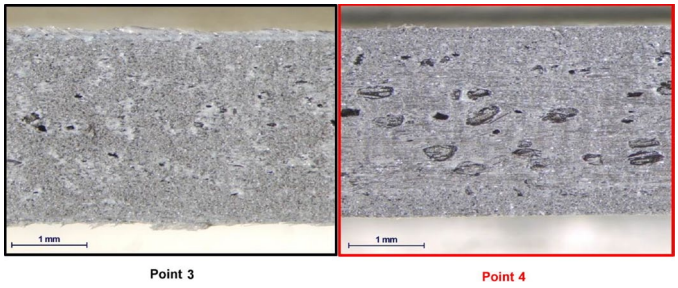


Fig. 4. The cross-section of the MuCell® part prepared on the microtome – points 3 and 4 as in Fig. 3

## 4. Conclusions

The microcellular foaming injection moulding process is an interesting non-conventional modification of the injection moulding process. The porous structure, created during this process, is dependent on the pressure of the molten plastic which is different in different mould cavity areas, dropping along the plastic flow direction. After literature research and analysis of the results presented in this article, the following conclusions were drawn:

– the degree of porosity of individual regions of the moulded part made with the MuCell® technology is not uniform.

The local porosity depends mainly on the injection process conditions and the nature of the material flow in the mould. Significant differences were found in the degree of gas bubble growth in different areas of the moulded part. A similar mechanism was observed during the study of the distribution of gas bubbles dimensions across the wall thickness of the part. For the region of the mould cavity filled first, the largest diameters of the bubbles were observed in the middle of the wall thickness. At the end of the plastic flow path, the largest bubble sizes were observed in the region of the greatest shear: between the mould wall and the centre of the part thickness.

– on the basis of the above conclusion, it can be concluded that the mechanical strength of the mouldings will be different, depending on the flow length (distance from the mould gate). In the places of high concentration of bubbles with large diameters will be lower than in the regions where there are fewer bubbles or they have a small diameter (e.g. the top layer of the molded part)
– thanks to the MuCell® technology, many properties are improved, despite the fact that it causes local weakening of the injected parts. Examples of quality improvements include greater flexibility, damping, vibration resistance and reduction of sink marks [3,5÷6,16].
– the properties of injected parts in MuCell® technology can be predicted since they depend on the porosity of the foamed material [6,7] and the porosity degree can be controlled by the processing conditions [5]. This means that, depending on the application, it is possible to produce parts with the desired properties. Unfortunately, microfoaming always reduces the strength of the material.
– although the influence of microfoaming on mechanical properties was mostly investigated and reported in the literature, there are also another aspects of porous material application. The porosity as well as its parameters: the size and number of pores can influence the thermal conductivity of the material. When producing parts from more insulating material some benefits like energy saving can be obtained and the tests of thermal properties of microfoamed injection moulded materials are the possible direction of the future research. The results of the research undertaken lately [17] show that modifying the microfoamed material with graphene effects in the modification of such properties like electromagnetic interference shielding and this means that the field of application of microcellular plastic materials can be extended.

**Acknowledments**

The authors wish to thank *Improdex Sp. z o.o. company* from Czechowice-Dziedzice in Poland for the possibility of manufacturing the injection moulded parts.

## REFERENCES

[1] M.-L. Wang, R.Y. Chang, C.-H. Hsu, Molding Simulation. Theory and Practice, Hanser Publishers, Munich, Cincinnati (2018).
[2] E. Dostatni, Recycling-oriented eco-design methodology based on decentralised artificial intelligence. Management and Production Engineering Review **9** (3), 79-89 (2018). DOI: https://doi.org/10.24425/119537
[3] Trexel. A guide to the MuCell microcellular foam injection molding process – T Series. Brochure of Trexel company. trexel.com
[4] CELLMOULD®. Foam injection molding for light-weight parts. Wittmann Battenfeld (2017).
[5] Ch. Shia-Chung, Soc. Plast. E. **10** (2009). 10.1002/spepro.000055
[6] E. Bociąga, Special methods of polymers injection moulding (in Polish), WNT, Warsaw (2008).
[7] D. Sykutera, P. Szewczykowski, M. Roch, Ł. Wajer, M. Grabowski, M. Bieliński, Polimery **63** (11-12), 743-749 (2018). DOI: https://doi.org/10.14314/polimery.2018.11.1
[8] M. Szostak, P. Krzywdzińska, M. Barczewski, Polimery **63** (2), 145-152 (2018). DOI: https://doi.org/10.14314/polimery.2018.2.8
[9] D. Dias, C. Peixoto, R. Marques, C. Araújo, D. Pereira. P. Costa, V. Paulo, S. Cruz, Int. J. Lightweight Mater. Manuf. **5**, 137-152 (2022). DOI: https://doi.org/10.1016/j.ijlmm.2021.11.005
[10] J. Xu, Soc. Plast E. **10**. (2009). 10.1002/spepro.000059
[11] G.-H. Hu, W. Yue, Microcellular Foam Injection Molding Process, In book: Some Critical Issues for Injection Molding (2012). DOI: https://doi.org/10.5772/34513
[12] E. Bociąga, P. Palutkiewicz, Microcellular Injection Moulding (in Polish) Polymer Processing / Przetwórstwo Tworzyw **4**, 309-317 (2013).
[13] S. Gong, M. Yuan, A. Chandra, H. Kharbas, A. Osorio, L.S. Turng, International Polymer Processing **2**, 202 (2005). DOI: https://doi.org/10.3139/217.1883
[14] M. Yuan, L.-S. Turng, Polymer **46**, 7273-7292 (2005). DOI: https://doi.org/10.1016/j.polymer.2005.06.054
[15] Q. Ren, M. Wu, Z. Weng, L. Wang, W. Zheng, Y. Hikima, M. Ohshima, J. CO2 Util. **48**, 101530 (2021). DOI: https://doi.org/10.1016/j.jcou.2021.101530
[16] L.J. Hyde, L. Kishbaugh, The MuCell® Injection Molding Process: A Strategic Cost Savings Technology for Electronic Connectors, Ticona Materials (2003).
[17] M. Hamidinejad, M. Salari, L. Ma, N. Moghimian, B. Zhao, H.K. Taylor, T. Filleter, C.B. Park, Carbon **187**, 153-164 (2022). DOI: https://doi.org/10.1016/j.carbon.2021.10.075